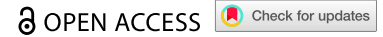










ORIGINAL RESEARCH



Anti-CD122 antibody restores specific CD8⁺ T cell response in nonalcoholic steatohepatitis and prevents hepatocellular carcinoma growth

Stéphanie Lacotte ^a, Florence Slits^a, Beat Moeckli ^{a,b}, Andrea Peloso ^{a,b}, Stéphane Koenig ^c, Matthieu Tihy ^d, Sofia El Hajji ^a, Quentin Gex^a, Laura Rubbia-Brandt ^d, and Christian Toso ^{a,b}

^aTransplantation and Hepatology Laboratory, Department of Surgery, University of Geneva, Geneva, Switzerland; ^bDivision of Abdominal Surgery, Department of Surgery, Geneva University Hospitals and Faculty of Medicine, Geneva, Switzerland; ^cDepartment of Physiology, University of Geneva, Geneva, Switzerland; ^dDivision of Clinical Pathology, Geneva University Hospitals and Faculty of Medicine, Geneva, Switzerland

ABSTRACT

Nonalcoholic steatohepatitis (NASH) can lead to hepatocellular carcinoma (HCC). Although immunotherapy is used as first-line treatment for advanced HCC, the impact of NASH on anticancer immunity is only partially characterized. We assessed the tumor-specific T cell immune response in the context of NASH. In a mouse model of NASH, we observed an expansion of the CD44⁺CXCR6⁺PD-1⁺CD8⁺ T cells in the liver. After intra-hepatic injection of RIL-175-LV-OVA-GFP HCC cells, NASH mice had a higher percentage of peripheral OVA-specific CD8⁺ T cells than control mice, but these cells did not prevent HCC growth. In the tumor, the expression of PD-1 on OVA-specific CD44⁺CXCR6⁺CD8⁺ cells was higher in NASH mice suggesting lowered immune activity. Treating mice with an anti-CD122 antibody, which reduced the number of CXCR6⁺PD-1⁺ cells, we restored OVA-specific CD8 activity, and reduced HCC growth compared to untreated NASH mice. Human dataset confirmed that NASH-affected livers, NASH tissues adjacent to HCC and HCC in patients with NASH exhibited gene expression patterns supporting mouse observations. Our findings demonstrate the immune system fails to prevent HCC growth in NASH, primarily linked to a higher representation of CD44⁺CXCR6⁺PD-1⁺CD8⁺ T cells. Treatment with an anti-CD122 antibody reduces the number of these cells and prevents HCC growth.

ARTICLE HISTORY

Received 8 June 2022
Revised 19 January 2023
Accepted February 22, 2023

KEYWORDS

Hepatocellular carcinoma;
immunotherapy;
nonalcoholic steatohepatitis

Introduction

Immune checkpoint inhibitors are one of the most encouraging treatment options for patients with hepatocellular carcinoma (HCC).¹ The combined use of atezolizumab (anti-PD-L1 antibody) and bevacizumab (VEGFA inhibitor) is now recognized as first-line treatment for advanced HCC.² However, the type of underlying liver disease, and specifically the presence of metabolic-related liver disease such as nonalcoholic fatty liver disease (NAFLD) and nonalcoholic steatohepatitis (NASH), can alter the immune profile and the response to the treatment. This will have a major impact on treatment selection considering that metabolic-related liver disease is on the way to become the leading cause of liver cancer in Western countries.³

Obesity, for example, has a paradoxical effect on tumors. Patients with a higher visceral fat area suffer more frequent HCC recurrence after treatment with radiofrequency ablation.⁴ In parallel, cancer patients with high body mass index have a better overall survival after immune checkpoint inhibitor therapy.^{5–7} In more advanced liver disease, the immune response against tumor-associated antigens is weaker in NASH-driven than in virus-driven HCC.⁸ NASH also reduces the efficiency of immunotherapeutic agents, such as antitumor vaccine and anti-OX40, to inhibit liver tumor growth by reducing tumor infiltration by CD4⁺ T cells in a HCC mouse model.⁹ Recently, Pfister et al. have suggested that NASH limits antitumor surveillance in immunotherapy-treated HCC (anti-

PD-1 antibody).¹⁰ These data highlight the importance of the etiology of HCC in the immune response and the efficiency of immunotherapies.

Activated T cells are known to be present in the liver during the development of metabolic liver disease even if the exact impact of CD4⁺ and CD8⁺ cells on the pathology is still debated.^{11,12} The discrimination between the T cells implicated in the underlying liver disease and the T cells directed against HCC antigens was usually restricted to a spatial assessment (tumor/peritumor/liver). To assess the cytotoxic immune response in HCC, we engineered an HCC cell line that expresses a non-self-antigen. This helped us differentiate the liver-infiltrating cells implicated in NASH and in the anti-HCC immune response.

Using a mouse model of NASH with HCC recurrence, we assessed the ability of the immune system to promote the anti-HCC immune response, the phenotype of the cells implicated in this immune response, and whether the depletion of the cells implicated in the underlying liver disease would improve the antitumor immunity. We also compared the human gene expression patterns of the markers identified in mice.

Materials and methods

Animal protocol

The animal research protocol was approved by the ethical committee at the University of Geneva and the Geneva

veterinary authorities (GE195/19 and GE71). All mice were housed in the animal facility of the University of Geneva on 12/12-hour light/dark cycles with free access to food and water. C57BL/6 N were purchased from Charles River Laboratories (Ecully, France) and were fed a control diet (ND: 17% kcal fat, 61% kcal carbohydrate, 22% kcal protein; Envigo TD.120455) or a high fat/high sucrose diet (HFD: 45% kcal fat, 41% kcal carbohydrate, 15% kcal protein; Envigo TD.08811) for 30 weeks. Mice underwent laparotomy and 1.5×10^5 RIL-175-LV-OVA-GFP or 4×10^5 MC-38 cells were injected into the portal vein. One group of HFD-fed mice was injected with 100 μ g of anti-CD122 antibody per mouse (intraperitoneal, 5H4, BioXcell) every third day starting on day 12 after HCC injection. The control group was injected with rat IgG2a. For CD8+ cells depletion, mice were injected with 150 μ g of anti-CD8a per mouse (intraperitoneal, 53-6.7, BioXcell) every third day starting on day 12 after HCC injection. For macrophages and dendritic cells depletion, HFD-fed mice were injected with clodronate liposomes (intraperitoneal, Liposoma) every four days starting on day 8 after HCC injection. PBS liposomes were injected as control.

Cell engineering

HCC cell line RIL-175 (gift from Prof. Tim Greten) was transduced with LV-EF-cOVA-IRES-GFP lentivirus. A LV-EF-cOVA-IRES-GFP lentivirus was constructed through insertion of the cytoplasmic ovalbumin (OVA) fragment (from pCI-neo-cOVA, gift from Dr. Maria Castro (Addgene plasmid #25097)) into pLOX-EW-iresGFP. A three-plasmid expression system was used to generate second-generation lentiviral vectors by transient transfection of 293 T cells (Lenti-X packaging Single Shots (VSV-G, Takara cat# 631275)). The transfection allowed constitutive cytoplasmic expression of the 143–383 OVA fragment and GFP.

Liver isolation

The hepatic non-parenchymal cells were isolated as previously described¹³. Briefly, the supra-hepatic inferior vena cava was cannulated, and the liver was perfused in a retrograde fashion with a wash solution (HBSS, EGTA 0.5 mM, HEPES 25 mM, penicillin-streptomycin 1 μ g/ml, glucose 0.1% and heparin 5 U/ml). Next, liver digestion was performed for 5 min (5 ml/min, 37°C, IMDM, Collagenase IV, Worthington at 0.5 mg/ml, and DNase I, Roche at 0.1 mg/ml). Digested livers were filtered on a 70 μ m nylon cell strainer. Hepatocytes were discarded after two 5-min centrifugations at 68 g, 4°C. Liver cell-rich fraction was separated by density gradient centrifugation (1400 g, slow acceleration nor brake) on OptiPrep 17.4%–8.2% (Sigma).

Flow cytometry

The liver cells were incubated with Fc-blocking reagent (TrueStain, Biolegend) for 5 min, incubated with APC-

SIINFEKL-H-2Kb dextramers (Immunotools) for 10 min and then stained with the appropriate antibodies detailed in the supplementary files. For the assessment of the MHC class I molecule Kb bound to the ovalbumin peptide SIINFEKL, RIL-175-LV-OVA-GFP or RIL-175-LV-GFP cells were left untreated or incubated overnight with 250 ng/ml γ IFN (Peprotec) and then labeled with the APC anti-SIINFEKL-H2Kb antibody (clone 25-D1.16). The samples were processed with an Attune NxT Cytometer (ThermoScientific) and analyzed with FloJo (Treestar). Results of FACS analysis are presented as the percentage of a population or as mean fluorescence index (MFI).

Antigen-specific proliferation assay

1×10^4 RIL-175-LV-OVA-GFP or RIL-175-LV-GFP cells were left untreated or incubated overnight with 250 ng/ml γ IFN (Peprotec). Lymph nodes and spleen cells were sorted, labeled with CFSE and incubated at different effector/target ratio with RIL-175 cells for 48 hours.

MRI

Formalin-fixed tumors-bearing livers that were not used for liver cell isolation were assessed by micro-MRI (Nanoscan 3 T, RS2D, Mundolsheim, France) with a birdcage coil of 3.5-cm diameter. After automatic adjustment of the B0 homogeneity, T1w and T2w images were acquired. MRI images were loaded to OsiriX DICOM Viewer and tumors' contours were manually marked on each slide. Volumes were then calculated using the inbuilt application.

Gene expression

After total RNA (cells sorted using BD FACSAria cell sorter or liver tissue) extraction (Promega), cDNA was synthesized by extending a mix of random primers with the High Capacity cDNA Reverse Transcription Kit in the presence of RNAase Inhibitor (Applied Biosystems). The relative quantity of each transcript was normalized to the expression of EEF1, HPRT and GAPDH. SYBR Green reagent was used for real-time PCR on the ABI Prism 7000 sequence detection system (Applied Biosystems) according to the manufacturer's instructions. Primer sequences are provided in the supplementary files.

Mouse and human expression datasets

The whole genome expression data used in this study are available under the accession numbers GSE113508 and GSE164760. Immune score assessment was performed as described by Yoshihara et al. using R (version 4.0.4, R Foundation for Statistical Computing, Vienna, Austria). HCC samples were considered to have a high immune score when the score was higher than the maximum value of the healthy control. None of the genes analyzed in this study were included in the calculation of the immune score.

Statistical analysis

Statistical analyses were performed using Prism 9 (GraphPad Software Inc., La Jolla, California, US). Data are expressed as median \pm interquartile range (IQR) and were compared using the nonparametric test (Mann-Whitney) unless specified otherwise.

Results

NASH livers host CXCR6⁺ PD-1⁺ CD8⁺ cell subset

After 35 weeks of high-fat diet (HFD), C57BL/6 N mice were obese (Figure 1a, 45.6 vs 52.9 g) and developed severe steatosis and limited inflammation (Figure 1b, NAS 0 vs 6). We observed a decrease in the CD4⁺ T cells (12.5 vs 8.9%) and an increase in CD8⁺ T cells (8.03 vs 16.75%) in the livers of the NASH mice (Figure 1c). The selective apoptosis of CD4⁺ T cells in livers with steatohepatitis has been previously described and is linked to HCC carcinogenesis.¹⁴

In addition to being over represented in the liver of HFD-fed mice, CD8⁺ T cells had an activated phenotype with expression of CD44, and expressed more CXCR6 (Figure 1d). CXCR6⁺ CD8⁺ T cells have been shown to be auto-aggressive T cells implicated in the pathology of NASH in a mouse model.¹⁵ CD44⁺ CXCR6⁺ CD8⁺ T cells were elevated in the livers of HFD-fed mice (Figure 1e, 23.45 vs 49.2%). This cell subset expressed more PD-1 in HFD-fed compared to ND-fed mice (Figure 1f right, MFI 903 vs 1175). No difference was observed in the expression of other activation markers and costimulation molecules (Figure 1f, left and data not shown). Surprisingly, the CD44⁺ CXCR6⁺ CD4⁺ cell subset was more represented in the livers of ND-fed compared to HFD-fed mice (Figure 1e, 74.35 vs 41.1%).

CXCL16-expressing myeloid cells are more represented in the livers of HFD-fed mice

CXCR6 binds exclusively to its ligand CXCL16.¹⁶ The expression of CXCL16 in the livers of HFD-fed mice correlated with the expression of CD8, indicating that this chemokine may directly attract CXCR6-expressing cells (Figure 2a, $r = 0.694$).

In addition to hepatocytes, liver sinusoidal endothelial cells (LSECs) and liver macrophages (Küpfner cells), the livers of HFD-fed mice hosted various subsets of myeloid cells (Figure 2b). Specifically, dendritic cells (CD11b⁺ CD11c⁺ CX3CR1⁺ MHC-II⁺ Gr1⁻, 3.6% in ND vs 9.5% in HFD), monocytes (CD11b⁺ CD11c⁺ CX3CR1⁺ MHC-II⁻, 3.1% in ND vs 5.1% in HFD) and monocytic myeloid-derived suppressor cells (MDSCs) (CD11b⁺ Gr1⁺ Ly6G⁻, 4.1% in ND vs 8.4% in HFD) were more represented in the liver of HFD-fed compared to ND-fed mice (Figure 2c, d). LSECs, macrophages and dendritic cells were the cell populations that expressed the highest levels of CXCL16 in HFD-fed mice (Figure 2b, 2.66 vs 3.18 vs 4.53 fold increase compared to hepatocytes). Of note, LSECs from ND- and HFD-fed mice expressed a similar level of CXCL16 (Supplementary Figure A) suggesting that the migration of CXCR6⁺ cells is promoted mainly by macrophages or invading myeloid cells such as dendritic cells and MDSCs, via their increased production of CXCL16.

Tumor antigen-specific T cells increase in circulating CD8⁺ T cells from HFD-fed mice

In order to assess whether the underlying liver steatosis and inflammation altered the T-cell immune response against tumor antigens, we engineered an HCC cell line (RIL-175) expressing a non-self antigen, a fragment of the ovalbumin protein (OVA 143–386) including the two MHC-restricted epitopes OVA 323–339 (ISQAVHAAHAEINEAGR) and OVA 257–264 (SIINFEKL). As many tumor cell lines, the RIL-175-LV-OVA-GFP only express H-2Kb and the SIINFEKL-H2Kb complex is detectable at the cell membrane following incubation with γ IFN (Figure 3a). The RIL-175-LV-OVA-GFP promoted the proliferation of CD8⁺ T cells isolated from OT-I mice with or without pre-incubation with γ IFN (Figure 3b).

In order to mimic HCC recurrence, RIL-175-LV-OVA-GFP were injected into the portal vein of ND- and HFD-fed mice. 14 days later, peripheral blood mononuclear cells (PBMCs) were analyzed. CD8⁺ T cells were less represented in the blood of HFD-fed mice compared to ND-fed mice and decreased further after HCC developed (Figure 3c, 6.79 vs 9.65%). The decrease in CD8⁺ cells was associated with an increase of the Gr1⁺ cell population in HFD-fed mice after HCC developed (Figure 3d and Supplementary Figure B, 27.6% vs 33.4%). Using SIINFEKL-H-2Kb dextramers, we were able to determine the amount of tumor-specific CD8⁺ T cells in PBMCs. Surprisingly, despite a lower percentage of CD8⁺ T cells, HFD-fed mice developed a higher percentage of SIINFEKL-specific CD8⁺ T cells (dextramers⁺ cells) detectable in PBMCs (Figure 3e, 3.6% vs 8.3%). The expression of CD69 was higher in the entire CD8⁺ T cells population of HFD-fed mice but the SIINFEKL-specific CD8⁺ T cells expressed a similar level of CD69 both in ND- and HFD-fed mice (Figure 3f, MFI 647 vs 613).

Tumor burden increased in HFD-fed mice

Three weeks after the RIL-175-LV-OVA-GFP injection, tumor burden was assessed. As demonstrated previously, the injured liver is more prone to HCC recurrence and tumor growth.^{7,17,18} In our model of steatohepatitis, tumor burden was increased in the liver of HFD-fed mice compared to ND-fed mice (Figure 4a-b, 1603 mm³ vs 620 mm³). The SIINFEKL-specific CD8⁺ T cells detectable in PBMCs were not able to modulate the tumor burden in HFD-fed mice. The immune cell composition of tumors and of the peritumoral livers were comparable to the compositions before HCC implantation, with a high presence of MDSCs, especially monocytic MDSCs (Figure 4c, 2.45% in ND vs 7.74% in HFD).

The underlying liver disease emphasize the exhaustion phenotype of tumor-specific cytotoxic T cells

The differences observed in the T cell subsets between HCC-bearing livers from ND- and HFD-fed mice were diminished (Figure 5a, 8.8% of CD4⁺ cells in ND vs 6.5% in HFD and 5.7% of CD8⁺ cells in ND vs 10.5% in HFD). CD8⁺ cells remained increased in the livers of HFD-fed mice but the presence of

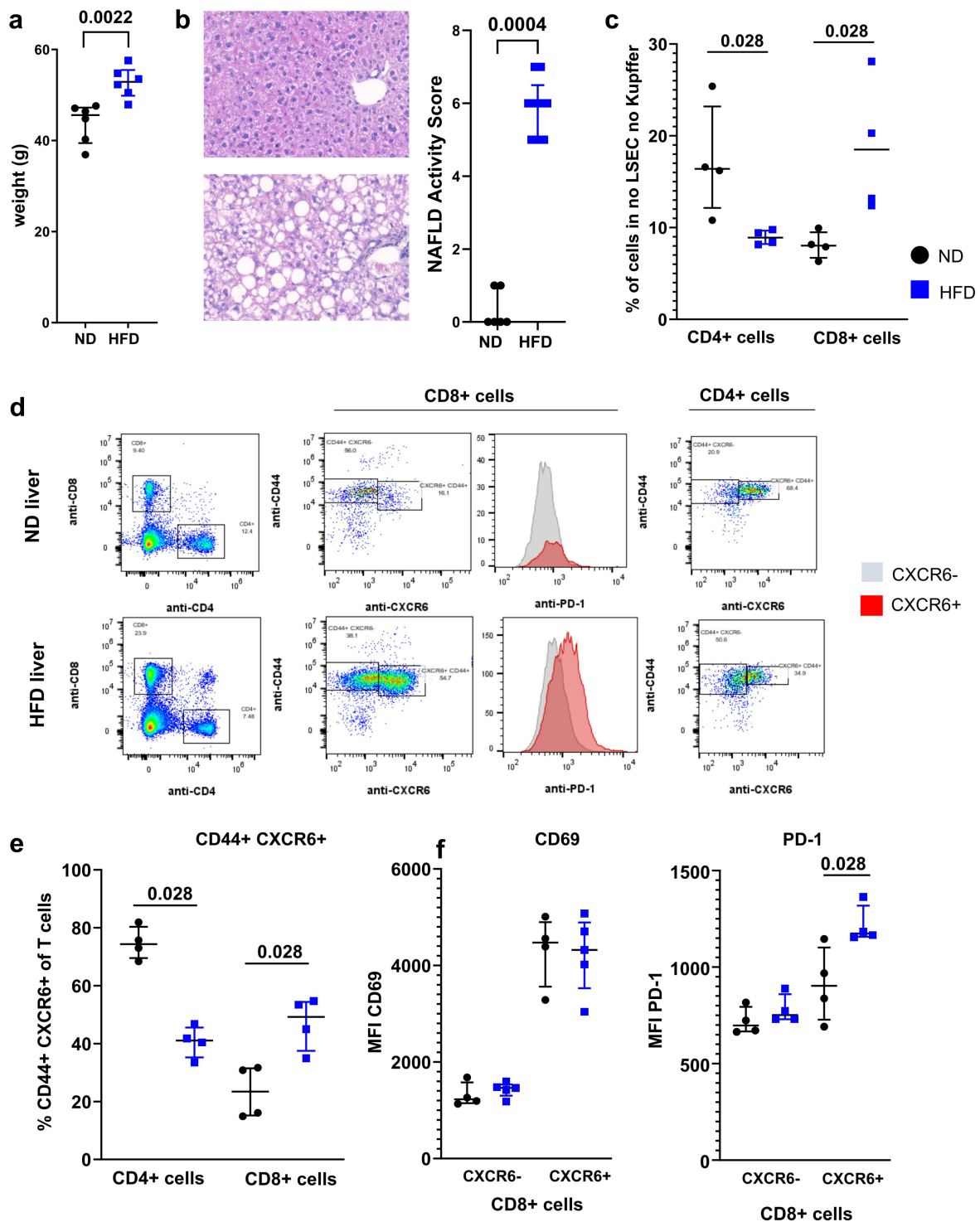


Figure 1. NASH altered T cells phenotype. A. Weight of C57BL/6 N mice following 30 weeks of HFD. B. Representative histology of liver of ND and HFD-fed mice at 35 weeks and assessment of NAFLD Activity Score. C. Representation of CD4 T cells and CD8 T cells in the liver of ND and HFD-fed mice. D. Phenotype of CD4 T cells and CD8 T cells isolated from livers of ND and HFD-fed mice. CD44⁺ CXCR6⁺ cells and their expression of PD-1 were assessed. E. Percentage of CD44⁺ CXCR6⁺ cells in the CD4 and CD8 T cell population in ND and HFD-fed mice. F. Expression level of CD69 (left) and CD279 (PD-1) in the CXCR6⁻ and CXCR6⁺ CD8 T cells subsets. A: n = 6 per group; B: n = 6 (ND) and n = 9 (HFD); C-F: n = 4 per group. Results are expressed as median and IQR.

tumor abolished the increase of CD44⁺ CXCR6⁺ cell subset previously observed in the CD8⁺ cell population (Figure 5b).

In order to assess the phenotype of the tumor-specific T cells, we analyzed the SIINFEKL-specific CD8⁺ T cells in the tumor and in the adjacent liver parenchyma (Figure 5c). We found no differences in the percentage of SIINFEKL-

specific CD8⁺ T cells (dextramers⁺ cells) in ND- and HFD-fed mice (Figure 5d, 12.3% vs 13.3%). Nearly all of the CD8⁺ dextramers⁺ cells were in the CD44⁺ CXCR6⁺ cell subset in both ND- and HFD-fed mice, meaning that both normal and steatotic livers were able to promote an antigen-specific immune response (Figure 5e, 87.8% vs 81.7%). However, the

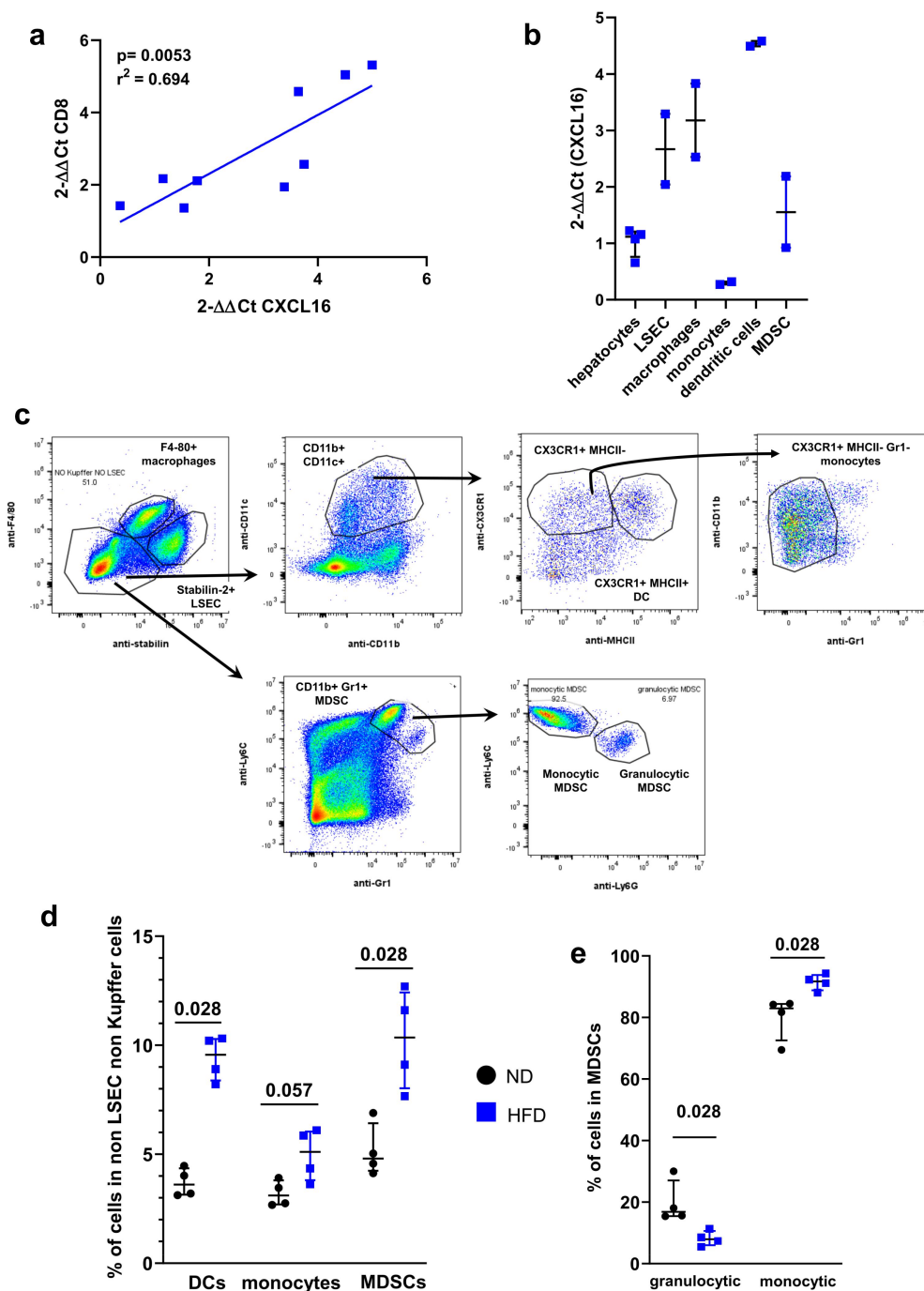


Figure 2. CXCL16-expressing myeloid cells are presented in NASH livers. **A.** Correlation between CXCL16 gene expression level and CD8 gene expression level in the liver of HFD-fed mice. **B.** Expression level of CXCL16 in sorted liver cell subsets from HFD-fed mice: hepatocytes, LSEC, macrophages, monocytes dendritic cells and MDSC. Results are expressed as $2^{-\Delta\Delta Ct}$ compared to hepatocytes. **C.** Representative gating strategy. **D.** Percentage of myeloid cells such as dendritic cells, monocytes and MDSCs in the liver of ND and HFD-fed mice. **E.** Representation of granulocytic and monocytic cell subsets in the MDSCs population in ND and HFD-fed mice. A: n = 9; B: n = 3 per group; D-E n = 4 per group. Results are expressed as median and IQR.

CD8⁺ dextramers⁺ cells from the livers of HFD-fed mice expressed a higher level of PD-1, suggesting a lower immune activity (Figure 5c and f, MFI 12605 vs. 16083). These results were confirmed using the GSE113508 dataset where the gene expression was evaluated in colorectal cancer injected into healthy or fatty livers.¹⁹ Colorectal cancer implanted into fatty livers had an increased expression of CXCL16, CXCR6, PD-L1 and PD-1 (Supplementary Figure C). Macrophages and dendritic cells are among the main producers of CXCL16. In order to assess their role in the migration of CD8⁺ CXCR6

+ cells, we depleted them with clodronate liposomes. However, while we achieved a successful depletion of macrophages (0.65% vs 7.97%) and dendritic cells (1.57% vs 9.33%), the migration of CD8⁺ CXCR6⁺ cells remained with no measurable change (12% vs 14.37 in total CD8⁺ CXCR6⁺ cells and 1.60% vs 1.79% in dextramers⁺ CXCR6⁺ cells). This observation suggest that macrophages and dendritic cells are not the only mediators for CXCR6-expressing cell migration into the liver. Interestingly, the depletion of macrophages and dendritic cells correlated with a decreased expression of PD-1 and

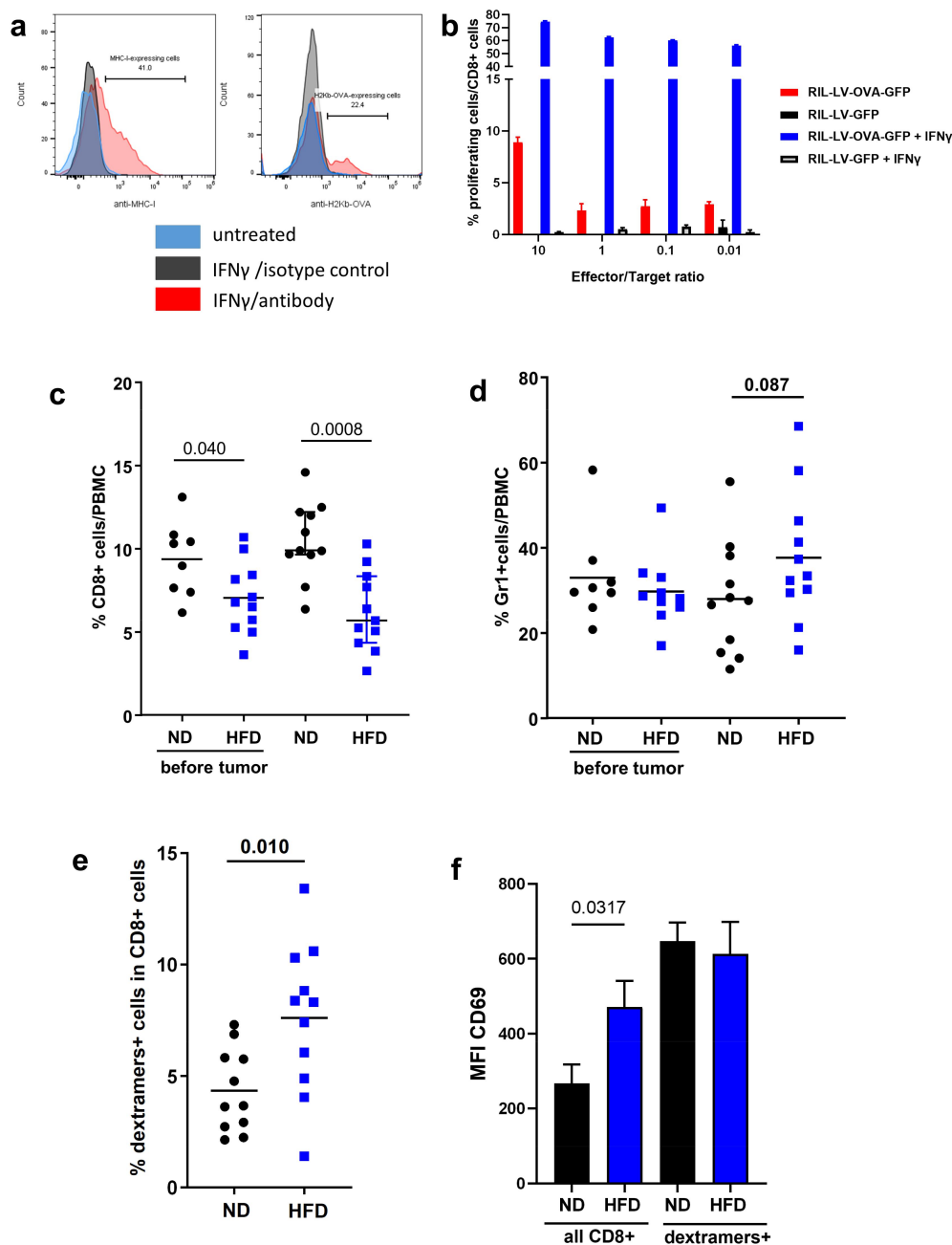


Figure 3. Construction of the HCC cell line RIL-175-LV-OVA-GFP and assessment of the OVA-specific immune response. A. Incubation with γ IFN potentiated the expression of MHC-I and the presentation of the SIINFEKL on H2Kb MHC-I in RIL-175-LV-OVA-GFP cells. B. Percentage of proliferation of CD8 T cells from OT-I mice after incubation with RIL-175-LV-OVA-GFP or RIL-175-LV-GFP cells with or without γ IFN. C. Assessment of CD8 T cells in the PBMC of ND and HFD-fed mice before and after intraportal injection of RIL-175-LV-OVA-GFP HCC cells. D. Assessment of Gr1⁺ cells in the PBMC of ND and HFD-fed mice before and after intraportal injection of RIL-175-LV-OVA-GFP HCC cells. E. Representation of SIINFEKL-specific CD8 T cells (dextramers⁺ cells) in the CD8 T cells from PBMC of ND and HFD-fed mice. F. Expression level of CD69 in the CD8 T cells and in the SIINFEKL-specific CD8 T cells (dextramers⁺ cells) from the PBMC of ND and HFD fed mice. C: n = 8 (ND before), n = 11 (HFD before), n = 11 (ND) and n = 11 (HFD); E-F: n = 11 per group. Results are expressed as median and IQR.

CD366 (Tim-3) both on CD8⁺ CXCR6⁺ cells and CD8⁺ dextramers⁺ cells (Supplementary Figure D).

Anti-CD122 treatment restores tumor-specific CD8⁺ T cells activity and decreases tumor burden

It has been suggested that the liver microenvironment in NASH limits the beneficial effect of immunotherapy (anti-PD-1) through the increase of CD8⁺ CXCR6⁺ PD-1⁺ cells.¹⁰ This cell subset is also known to promote NASH lesions and that

CXCR6⁺ PD-1^{high} CD8⁺ T cells originate from CD122-expressing T cells.¹⁵ Anti-CD122 treatment reduced CXCR6⁺ CD8⁺ T cells expressing a high level of PD-1 and restored hepatic function in NASH.¹⁵ We assessed whether this treatment is also able to promote antitumor immunity through the depletion of CD8⁺ CXCR6⁺ PD-1⁺ cells in HFD-fed mice with HCC.

Three days after the first anti-CD122 injection, CD8⁺ cells were increased in the blood of HFD-fed mice compared to untreated HFD-fed mice (Figure 6a, 8.5% in treated HFD vs

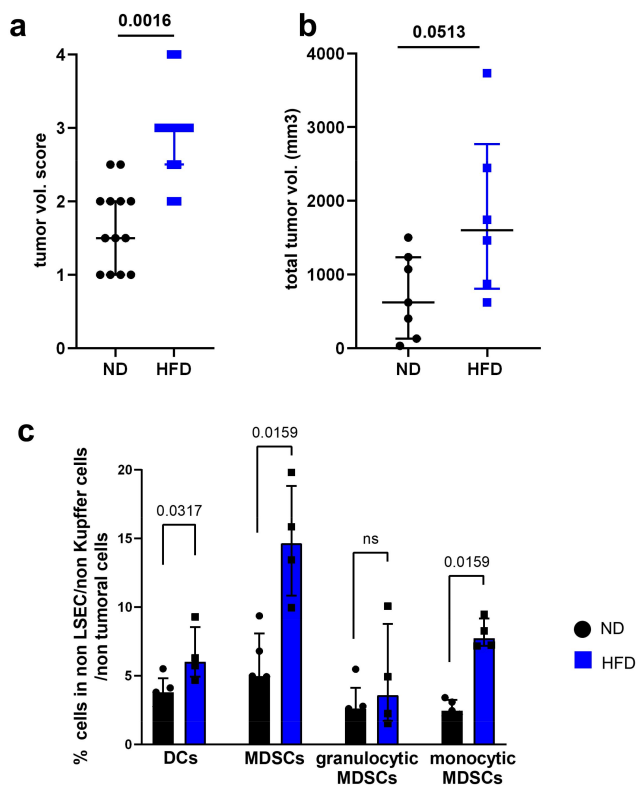


Figure 4. Tumor burden increased in mice with NASH. A. Tumor growth was macroscopically assessed with a score from 0 to 4 (0 = no tumor, 1 = less than 5 small nodules (<2 mm), 2 = more than 5 small nodules (<2 mm) or one medium nodule (>2 mm – <5 mm), 3 = more than 1 medium nodule, 4 = complete liver invasion). B. MRI assessment of total tumor volume on formal-fixed livers from ND and HFD-fed mice. C. Representation of myeloid cells subsets in the peritumoral liver from ND and HFD- mice. A: n = 13 (ND) and n = 12 (HFD); B: n = 7 (ND) and n = 6 (HFD); C: n = 5 per group. Results are expressed as median and IQR.

6.0% in HFD). The percentage of SIINFEKL-specific CD8⁺ T cells remained stable (dextramer⁺) (Figure 6b, 7.5% in treated HFD vs 8.1% in HFD). Anti-CD122-treated mice had fewer tumor nodules in the liver (Figure 6c, 2 in ND vs 11.5 in HFD vs 4.5 in treated HFD). The HCC nodules also had a tendency to be smaller in treated HFD-fed mice compared to untreated HFD-fed mice (Figure 6d). This effect was CD8⁺ T cells-specific, as the CD8-depleted anti-CD122-treated mice developed a similar amount of tumor nodules as the CD8-depleted mice, and both groups showed an increased tumor burden compared to non CD8-depleted mice (Figure 6e, 30 in CD8-depleted HFD vs 26.5 in CD8-depleted treated HFD). Similar amounts of CD44⁺ CXCR6⁺ CD8⁺ cells were present in ND-, HFD- and treated HFD-fed mice but the percentage of SIINFEKL-specific CD8⁺ T cells (dextramer⁺) increased in mice injected with the antibody (figure 6f, 0.77% in ND vs 1.49% in HFD vs 2.21% in treated HFD). These tumor-specific CD8⁺ T cells had reduced expression of PD-1 compared to cells from untreated HFD-fed mice suggesting that the antitumor activity was restored (Figure 6g, MFI 12605 in ND vs 16406 in HFD vs 19492 in treated HFD). The injection of anti-CD122 was tested in the model of colon adenocarcinoma MC-38 cells injected in the liver of HFD-fed mice. The treated HFD-fed mice developed less tumor nodules than the HFD-fed mice. However, this did not reach the significance as many mice did not develop tumors (Supplementary Figure G).

NASH livers and HCC in patients with NASH develop a similar immune signature

We next sought to validate our findings in a human cohort. The GSE164760 dataset contains expression data from liver biopsies of NASH, NASH adjacent to HCC and HCC associated with NASH. In human, nearly 30% of HCCs present markers of an inflammatory response (Immune Class) associated with better survival.²⁰ In HCC with etiologies other than NASH, the intratumoral immune profile differs from the surrounding non-tumoral liver.²⁰ In human, Immune Class of HCC could correspond to the phenotype of the underlying liver disease. An immune enrichment score, described by Yoshihara *et al.*, was applied on the studied HCC samples, allowing to discriminate between low and high immune score samples.²¹ As previously reported, 35% (19/53) of NASH-driven HCCs were considered to have “high immune score” (Supplementary Figure H). Similarly to what was observed in the mouse model, CD4 expression was lower in NASH tissue adjacent to HCC and HCC itself compared to the healthy liver (Figure 7 and Supplementary Figure H). The probe sets used to analyze the gene expression allowed a specific detection of two mRNA splice variants of the CD8B gene. The variant M-1, which is more expressed in naïve CD8⁺ T cells, was decreased in all groups compared to healthy controls.²² In contrast, the mRNA M-4 variant, known to be more expressed in effector memory T cells, had higher expression levels in NASH liver adjacent to HCC and in HCC with high immune score (Figure 7). We next investigated the expression patterns of genes associated with the phenotype we observed in mice. As in the mouse model, CXCL16 expression was increased in NASH-affected livers, NASH-affected livers adjacent to HCC and HCC with a high immune score compared to healthy livers (Figure 7, 433 vs 613 vs 710 vs 768). The expression of CD44 and CXCR6 tended to be higher in livers with NASH without reaching statistical significance, but their expression was significantly increased in NASH livers adjacent to HCC and in HCC with high immune score (Figure 7). These results indicate that CXCR6-expressing effector CD8⁺ T cells attracted to the liver via CXCL16 are implicated in NASH and HCC. We also tested the expression of the PD-1 gene PDCD1 but we found no difference in expression between the groups with none of the probe sets referenced for this gene.

Discussion

Our results demonstrate that mice with steatohepatitis do not impede a cytotoxic tumor-specific immune response with tumor-specific CD8⁺ T cells, which are detectable in the blood and in the peritumoral tissue. However, the disturbed liver microenvironment alters the activity of these CD44⁺ CXCR6⁺ CD8⁺ cells resulting in enhanced tumor growth.

Our results confirmed in part what was observed by J. McVey *et al.*, in a methionine choline deficient mouse model with antigen-presenting HCC cells.²³ They demonstrated that NAFLD mice have no inhibition on the generation of tumor antigen-specific CD8⁺ T cells, but found no increase in the PD-1 expression between normal and NAFLD livers. Our observed increase in PD-1 expression can be explained by

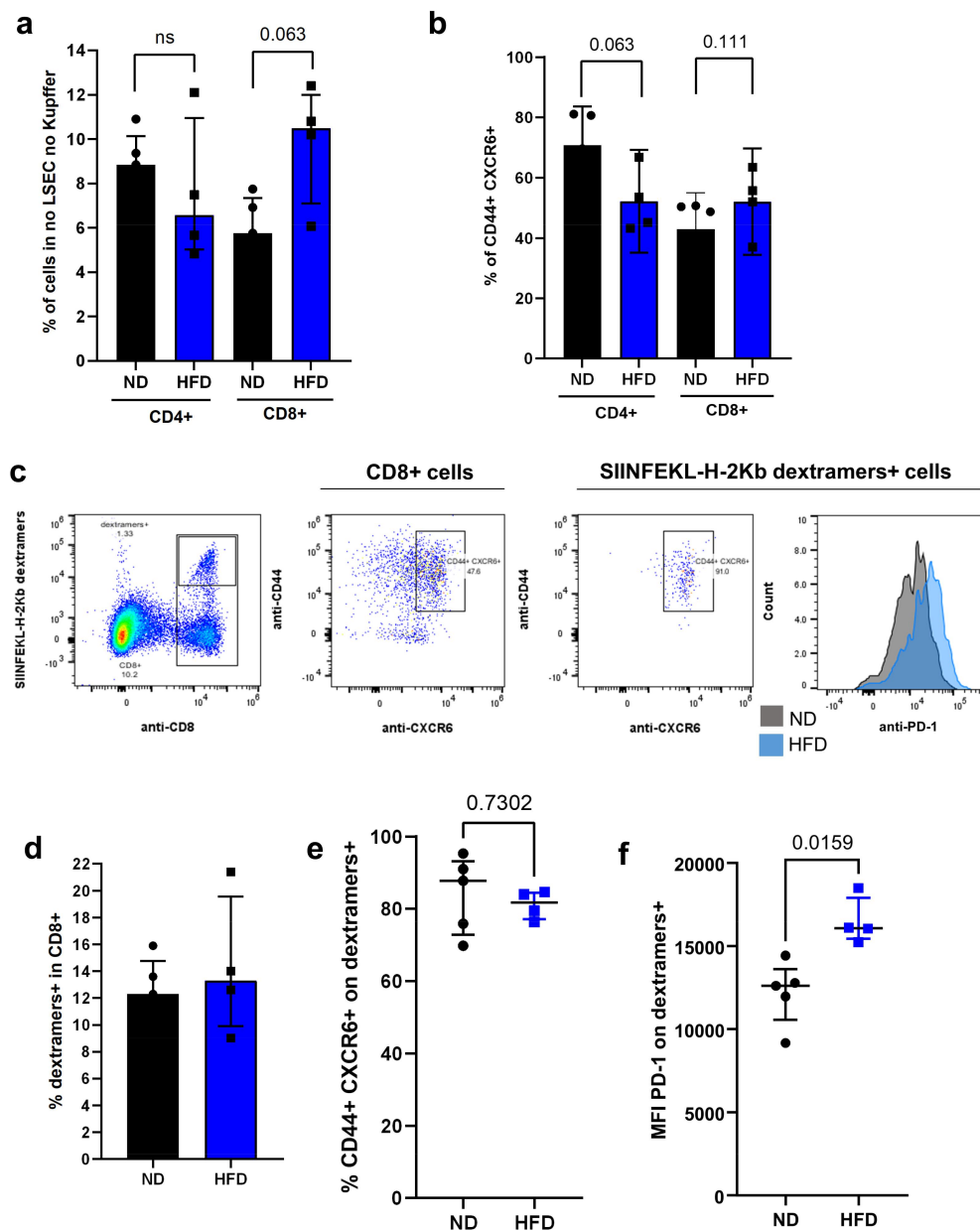


Figure 5. Tumor-specific CD8 T cells had an altered phenotype in NASH mice. A. Representation of CD4 T cells and CD8 T cells in the liver of HCC-bearing ND and HFD-fed mice. B. Percentage of CD44⁺ CXCR6⁺ cells in the CD4 and CD8 T cell population in HCC-bearing ND and HFD-fed mice. C. Phenotype of CD8 T cells and SIINFEKL-specific CD8 T cells (dextramers+ cells) from the liver of HCC-bearing mice. D. Percentage of SIINFEKL-specific CD8 T cells (dextramers+ cells) in the CD8 T cells from the liver of ND and HFD-fed mice. E. Percentage of CD44⁺ CXCR6⁺ in SIINFEKL-specific CD8 T cells (dextramers+ cells) from the liver of HCC bearing ND and HFD-fed mice. F. Expression level of CD279 (PD-1) on SIINFEKL-specific CD8 T cells (dextramers+ cells) from the liver of HCC bearing ND and HFD-fed mice. A-F: n = 5 (ND), n = 4 (HFD). Results are expressed as median and IQR.

a different experimental setup (HCC cell line, diet, tumor cell isolation) but also by the fact they did not focus on CD44⁺ CXCR6⁺ cells, which are the PD-1-expressing cell subset. This study also highlighted the role of macrophages, which impede for the antigen-specific anti-tumor immunity in the disturbed hepatic environment.

The infiltration of myeloid cells in the HCC predicts the prognosis of the disease.²⁴ However, it has always been ambiguous whether this increase is a cause or a consequence of tumor growth. In our model, NASH led to an increase in dendritic cells, macrophages and monocytic MDSCs in the liver, with no further contribution from the tumor. CXCL16 has been shown to be produced by

different cell types: LSECs,²⁵ hepatocytes and macrophages,²⁶ dendritic cells²⁷ and monocytic MDSCs.²⁸ In our experiments, mainly dendritic cells and macrophages produced CXCL16 and its secretion attracted CXCR6 CD8⁺ T cells into the liver and into the tumor. The CXCL16-CXCR6 axis explains the attraction of CXCR6-expressing cells into the liver but not their altered phenotype. The liver NASH microenvironment by itself can be responsible for the alteration. For example, the lack of response to anti-PD-1 treatment in NASH has been related the migration of CXCR2-expressing neutrophil with a protumour phenotype.²⁹ Liver CD8⁺ T cells from a mouse model of NASH with HCC have an impaired mitochondrial fitness

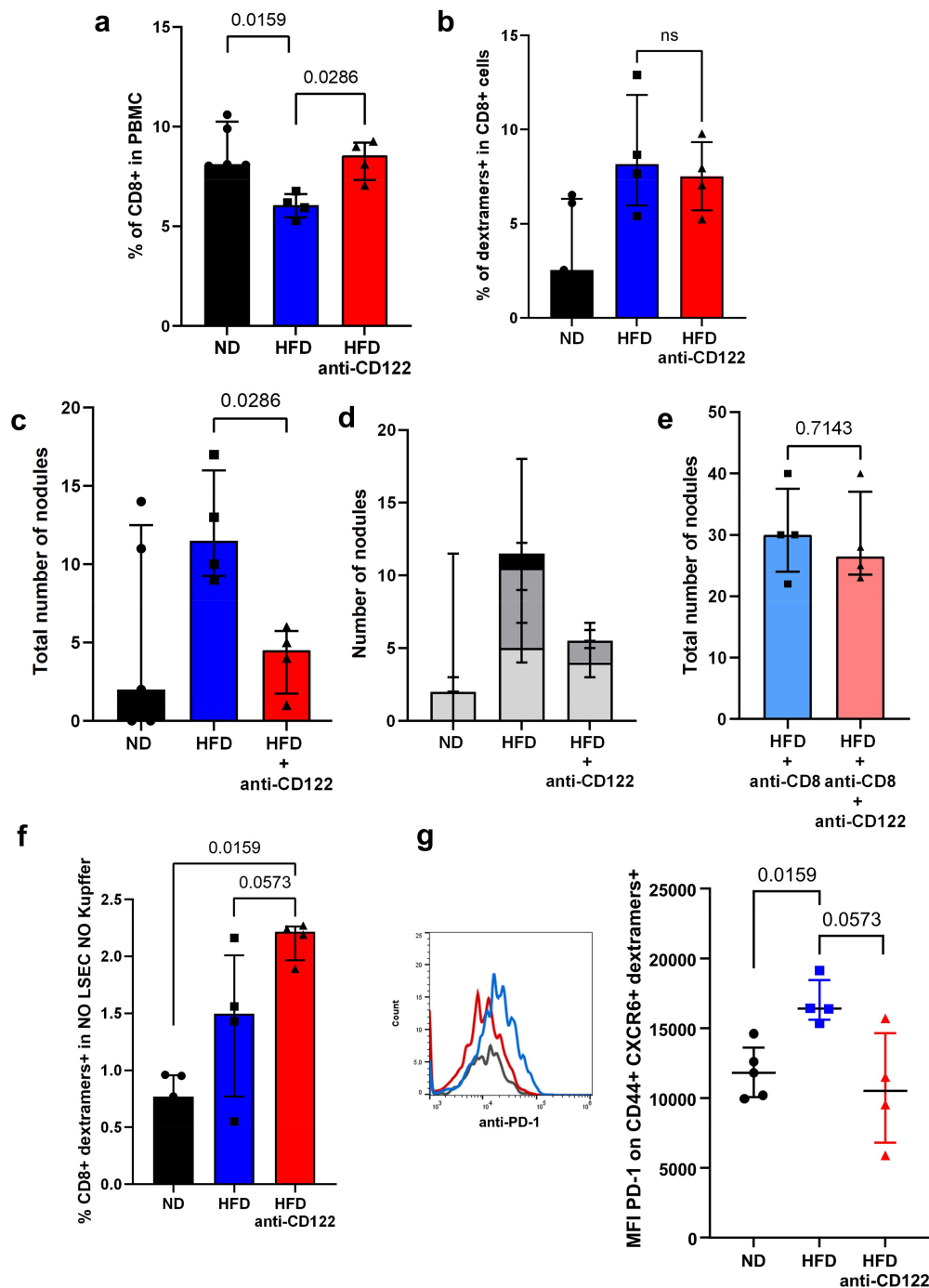


Figure 6. Anti-CD122 antibodies injection restored tumor-specific T cells phenotype. A. Representation of CD8 T cells in the PBMC of HCC-bearing mice. B. Percentage of SIINFEKL-specific CD8 T cells (dextramers+ cells) in the CD8 T cells from the PBMC of HCC-bearing mice. C. Assessment of the number of HCC nodules on the liver of mice. D. Assessment of the number and the size of the nodules on the liver of mice. Light gray = nodules < 1 mm, dark gray = nodules > 1 mm and < 3 mm; black = nodules > 3 mm. E. Assessment of the number of HCC nodules on the liver of mice. F. Percentage of SIINFEKL-specific CD8 T cells (dextramers+ cells) in PBMC of HCC-bearing mice. G. Expression level of CD279 (PD-1) on SIINFEKL-specific CD8 T cells (dextramers+ cells) in the liver of HCC-bearing mice. A-G: n = 5 (ND), n = 4 (HFD, HFD + anti-CD122, HFD + anti-CD (and HFD + anti-CD8 + anti-CD122)). Results are expressed as median and IQR.

and a decreased motility. This phenotype has been shown to be rescued by a metformin treatment.³⁰ CD4⁺ T cells are also implicated in the development of NAFLD at the beginning of the disease.³¹ However the progression of NASH and the accumulation of toxic lipids lead to the depletion of CD4⁺ T cells that disturb the immune surveillance against HCC.^{9,14} Our data supports the depletion model and the lack of helper T cells could be implicated in the altered phenotype of CD8⁺ T cells.

In a recent study assessing the molecular characteristics of HCC in patients with NASH, NASH-HCC showed a higher prevalence of an immunosuppressive carcinogenic cancer field with signatures of responses to anti-PD-1 therapies in non-cirrhotic NASH-HCC.³² We found higher expression of PD-1 in tumor-specific T cells. Currently, NASH-driven HCC would be considered a candidate for immune checkpoint therapy. However, NASH-driven HCC might be less responsive to anti-PD-1 treatment, probably owing to the dysregulated NASH-

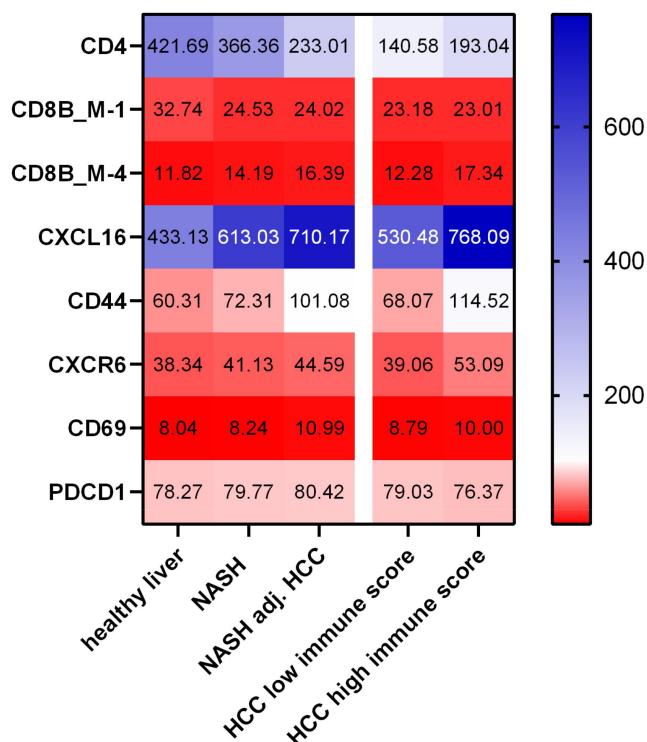


Figure 7. NASH livers and HCC in patients with NASH develop a similar immune signature. Heat map of gene expression in healthy livers (n =6), livers with NASH (n =74), livers with NASH adjacent to HCC (n =29), HCC with low immune score (n =34) and HCC with high immune score (n =19). Results are expressed as median.

specific T cell activation causing tissue damage.¹⁰ In accordance with what is suggested in the literature, the results from the gene expression datasets both in mice and human indicate that the immune response against liver cancer is at least partially linked to the underlying parenchyma.³²

In our experiments, the depletion of the precursors of CXCR6⁺ PD-1^{high} CD8⁺ T cells via the anti-CD122 antibody treatment increased the tumor-specific T cells and restored lower expression of PD-1. This was associated with a decreased tumor burden in anti-CD122-treated animals. Of note, anti-CD122 treatment had no effect on hepatic enzymes (Supplementary Figure E).

The observed decrease in HCC growth may be the consequence of the restoration of the activity of tumor-specific CD8⁺ T cells but it cannot be excluded that the anti-CD122 antibody acted on the tumor through other mechanisms. In a mouse model of melanoma, targeting CD122 enhanced the inflammatory cytokine production from CD8⁺ cells and the antitumor immunity.³³ CD122 was also demonstrated to be present on CD8⁺ regulatory T cells in HCC and the depletion of these cells lead to an increase antitumor immunity.³⁴

Our study had some limitations, as we assessed a strong antigenic immune response far from the tumor-associated antigens. The sequences of epitopes and the levels of antigens play a crucial role in the development of the hepatic immune response.^{8,35} However, we were able to detect T cells with an exhausted phenotype and the tolerogenicity of ovalbumin in the context of liver immunity has been described in previous studies.^{35,36} Another limitation was the use of the HCC

recurrence model, where the implantation of high number of cells is different of what is observed during carcinogenesis. The targeting of CD122, also known as IL-2Rb or IL-15Rb, in cancer treatment should be considered cautiously and limited to the case of underlying inflammatory liver diseases. The signaling through CD122 as a component of the high-affinity IL-15 receptor is critical for costimulation-independent memory CD8⁺ T cell recall.³⁷ The clinical use of anti-CD122 in the case of tumors requiring the promotion of antigen-specific T cell response is challenging and would require more investigations. Altogether, the presented data reinforce the hypothesis that NASH alters the antitumor cytotoxic immune response through CD44⁺ CXCR6⁺ CD8⁺ T cells with high expression of PD-1. The antitumor response may be restored through the depletion of these cells with an anti-CD122 antibody, without worsening the underlying NASH disease.

Acknowledgments

We thank the team of the Flow cytometry, Genomic and Histology core facilities, as well as the small animal preclinical imaging platform facility of the Faculty of Medicine (University of Geneva). We thank Dr Nicolas Goossens for his advice and Dr Beata Kusmider for her attentive proofreading.

Disclosure statement

The authors report there are no competing interests to declare.

Funding

This work was supported by the Swiss National Science Foundation (grant number 182471), the “Fondation Francis & Marie-France Minkoff” and the Leenaards Foundation (grant number 5489).

ORCID

Stéphanie Lacotte <http://orcid.org/0000-0002-5921-6389>
 Beat Moeckli <http://orcid.org/0000-0002-9020-8416>
 Andrea Peloso <http://orcid.org/0000-0002-3089-0230>
 Stéphane Koenig <http://orcid.org/0000-0002-0801-279X>
 Matthieu Tihy <http://orcid.org/0000-0002-9314-4657>
 Sofia El Hajji <http://orcid.org/0000-0002-3028-6148>
 Laura Rubbia-Brandt <http://orcid.org/0000-0002-3173-3376>
 Christian Toso <http://orcid.org/0000-0003-1652-4522>

Data repository

The datasets analyzed during the current study are available in the Gene Expression Omnibus repository <https://www.ncbi.nlm.nih.gov/geo/>. The data that support the findings of this study are openly available in Yareta - 10.26037/yareta:3527i5vapbcmlmt2kob4v2r4hi

References

- Pinter M, Jain RK, Duda DG. The Current Landscape of Immune Checkpoint Blockade in Hepatocellular Carcinoma: a Review. *JAMA Oncol.* 2021;7(1):113–123. doi:10.1001/jamaoncol.2020.3381.
- Bruix J, Chan SL, Galle PR, Rimassa L, Sangro B. Systemic treatment of hepatocellular carcinoma: an EASL position paper. *J Hepatol.* Jul 10 2021. doi: 10.1016/j.jhep.2021.07.004

3. Goldberg D, Ditah IC, Saeian K, Lalehzari M, Aronsohn A, Gorospe EC, Charlton M. Changes in the Prevalence of Hepatitis C Virus Infection, Nonalcoholic Steatohepatitis, and Alcoholic Liver Disease Among Patients With Cirrhosis or Liver Failure on the Waitlist for Liver Transplantation. *Gastroenterology*. 2017;152(5):1090–1099.e1. doi:10.1053/j.gastro.2017.01.003.
4. Ohki T, Tateishi R, Shiina S, Goto E, Sato T, Nakagawa H, Masuzaki R, Goto T, Hamamura K, Kanai F, et al. Visceral fat accumulation is an independent risk factor for hepatocellular carcinoma recurrence after curative treatment in patients with suspected NASH. *Gut*. 2009;58(6):839–844. doi:10.1136/gut.2008.164053.
5. Cortellini A, Bersanelli M, Buti S, Cannita K, Santini D, Perrone F, Giusti R, Tiseo M, Michiara M, Di Marino P, et al. A multicenter study of body mass index in cancer patients treated with anti-PD-1/PD-L1 immune checkpoint inhibitors: when overweight becomes favorable. *J Immunother Cancer*. 2019;7(1):57. doi:10.1186/s40425-019-0527-y.
6. Kichenadasse G, Miners JO, Mangoni AA, Rowland A, Hopkins AM, Sorich MJ. Association Between Body Mass Index and Overall Survival With Immune Checkpoint Inhibitor Therapy for Advanced Non-Small Cell Lung Cancer. *JAMA Oncol*. 2020;6(4):512–518. doi:10.1001/jamaoncol.2019.5241.
7. Wang Z, Aguilar EG, Luna JJ, Dunai C, Khuat LT, Le CT, Mirsoian A, Minnar CM, Stoffel KM, Sturgill IR, et al. Paradoxical effects of obesity on T cell function during tumor progression and PD-1 checkpoint blockade. *Nat Med*. 2019;25(1):141–151. doi:10.1038/s41591-018-0221-5.
8. Inada Y, Mizukoshi E, Seike T, Tamai T, Iida N, Kitahara M, Yamashita T, Arai K, Terashima T, Fushimi K, et al. Characteristics of Immune Response to Tumor-Associated Antigens and Immune Cell Profile in Patients With Hepatocellular Carcinoma. *Hepatology*. 2019;69(2):653–665. doi:10.1002/hep.30212.
9. Heinrich B, Brown ZJ, Diggs LP, Vormehr M, Ma C, Subramanyam V, Rosato U, Ruf B, Walz JS, McVey JC, et al. Steatohepatitis Impairs T-cell-Directed Immunotherapies Against Liver Tumors in Mice. *Gastroenterology*. 2021;160(1):331–345.e6. doi:10.1053/j.gastro.2020.09.031.
10. Pfister D, Núñez NG, Pinyol R, Govaere O, Pinter M, Szydlowska M, Gupta R, Qiu M, Deczkowska A, Weiner A, et al. NASH limits anti-tumour surveillance in immunotherapy-treated HCC. *Nature*. 2021;592(7854):450–456. doi:10.1038/s41586-021-03362-0.
11. Sutti S, Jindal A, Locatelli I, Vacchiano M, Gigliotti L, Bozzola C, Albano E. Adaptive immune responses triggered by oxidative stress contribute to hepatic inflammation in NASH. *Hepatology*. 2014;59(3):886–897. doi:10.1002/hep.26749.
12. Breuer DA, Pacheco MC, Washington MK, Montgomery SA, Hasty AH, Kennedy AJ. CD8+ T cells regulate liver injury in obesity-related nonalcoholic fatty liver disease. *Am J Physiol - Gastrointest Liver Physiol*. 2020;318(2):G211–G224. doi:10.1152/ajpgi.00040.2019.
13. Meyer J, Lacotte S, Morel P, Gonelle-Gispert C, Bühler L. An optimized method for mouse liver sinusoidal endothelial cell isolation. *Exp Cell Res*. 2016;349(2):291–301. doi:10.1016/j.yexcr.2016.10.024.
14. Ma C, Kesarwala AH, Eggert T, Medina-Echeverez J, Kleiner DE, Jin P, Stroncek DF, Terabe M, Kapoor V, ElGindi M, et al. NAFLD causes selective CD4+ T lymphocyte loss and promotes hepatocarcinogenesis. *Nature*. 2016;531(7593):253–257. doi:10.1038/nature16969.
15. Dudek M, Pfister D, Donakonda S, Filpe P, Schneider A, Laschinger M, Hartmann D, Hüser N, Meiser P, Bayerl F, et al. Auto-aggressive CXCR6+ CD8 T cells cause liver immune pathology in NASH. *Nature*. 2021;592(7854):444–449. doi:10.1038/s41586-021-03233-8.
16. Matloubian M, David A, Engel S, Ryan JE, Cyster JG. A transmembrane CXC chemokine is a ligand for HIV-coreceptor Bonzo. *Nat Immunol*. 2000;1(4):298–304. doi:10.1038/79738.
17. Orci LA, Berney T, Majno PE, Lacotte S, Oldani G, Morel P, Mentha G, Toso C. Donor characteristics and risk of hepatocellular carcinoma recurrence after liver transplantation. *Br J Surg*. 2015;102(10):1250–1257. doi:10.1002/bjs.9868.
18. Oldani G, Crowe LA, Orci LA, Slits F, Rubbia-Brandt L, de Vito C, Morel P, Mentha G, Berney T, Vallée J-P, et al. Pre-retrieval reperfusion decreases cancer recurrence after rat ischemic liver graft transplantation. *J Hepatol*. 2014;61(2):278–285. doi:10.1016/j.jhep.2014.03.036.
19. Iwamoto H, Abe M, Yang Y, Cui D, Seki T, Nakamura M, Hosaka K, Lim S, Wu J, He X, et al. Cancer Lipid Metabolism Confers Antiangiogenic Drug Resistance. *Cell Metab*. 2018;28(1):104–117.e5. doi:10.1016/j.cmet.2018.05.005.
20. Sia D, Jiao Y, Martinez-Quetglas I, Kuchuk O, Villacorta-Martin C, Castro de Moura M, Putra J, Camprecios G, Bassaganyas L, Akers N, et al. Identification of an Immune-specific Class of Hepatocellular Carcinoma, Based on Molecular Features. *Gastroenterology*. 2017;153(3):812–826. doi:10.1053/j.gastro.2017.06.007.
21. Yoshihara K, Shahmoradgoli M, Martínez E, Vegesna R, Kim H, Torres-Garcia W, Treviño V, Shen H, Laird PW, Levine DA, et al. Inferring tumour purity and stromal and immune cell admixture from expression data. *Nat Commun*. 2013;4(1):2612. doi:10.1038/ncomms3612.
22. Thakral D, Dobbins J, Devine L, Kavathas PB. Differential expression of the human CD8beta splice variants and regulation of the M-2 isoform by ubiquitination. *J Immunol Baltim Md 1950*. 2008;180(11):7431–7442. doi:10.4049/jimmunol.180.11.7431.
23. McVey JC, Green BL, Ruf B, McCallen JD, Wabitsch S, Subramanyam V, Diggs LP, Heinrich B, Greten TF, Ma C. NAFLD indirectly impairs antigen-specific CD8+ T cell immunity against liver cancer in mice. *iScience*. 2022;25(2):103847. doi:10.1016/j.isci.2022.103847.
24. Wu C, Lin J, Weng Y, Zeng D-N, Xu J, Luo S, Xu L, Liu M, Hua Q, Liu C-Q, et al. Myeloid signature reveals immune contexture and predicts the prognosis of hepatocellular carcinoma. *J Clin Invest*. 2020;130(9):4679–4693. doi:10.1172/JCI135048.
25. Ma C, Han M, Heinrich B, Fu Q, Zhang Q, Sandhu M, Agdashian D, Terabe M, Berzofsky JA, Fako V, et al. Gut microbiome-mediated bile acid metabolism regulates liver cancer via NKT cells. *Science*. 2018;360(6391):eaan5931. doi:10.1126/science.aan5931.
26. Heydtmann M, Lalor PF, Eksteen JA, Hübscher SG, Briskin M, Adams DH. CXC Chemokine Ligand 16 Promotes Integrin-Mediated Adhesion of Liver-Infiltrating Lymphocytes to Cholangiocytes and Hepatocytes within the Inflamed Human Liver. *J Immunol*. 2005;174(2):1055–1062. doi:10.4049/jimmunol.174.2.1055.
27. Veinotte L, Gebremeskel S, Johnston B. CXCL16-positive dendritic cells enhance invariant natural killer T cell-dependent IFN γ production and tumor control. *Oncoimmunology*. 2016;5(6):e1160979. doi:10.1080/2162402X.2016.1160979.
28. Zhao W, Xu Y, Xu J, Wu D, Zhao B, Yin Z, Wang X. Subsets of myeloid-derived suppressor cells in hepatocellular carcinoma express chemokines and chemokine receptors differentially. *Int Immunopharmacol*. 2015;26(2):314–321. doi:10.1016/j.intimp.2015.04.010.
29. Leslie J, Mackey JBG, Jamieson T, Ramon-Gil E, Drake TM, Fercq F, Clark W, Gilroy K, Hedley A, Nixon C, et al. CXCR2 inhibition enables NASH-HCC immunotherapy. *Gut*. 2022 Apr 24;7110:2093–2106. doi:10.1136/gutjnl-2021-326259.
30. Wabitsch S, McCallen JD, Kamenyeva O, Ruf B, McVey JC, Kabat J, Walz JS, Rotman Y, Bauer KC, Craig AJ, et al. Metformin treatment rescues CD8+ T-cell response to immune checkpoint inhibitor therapy in mice with NAFLD. *J Hepatol*. 2022;77(3):748–760. doi:10.1016/j.jhep.2022.03.010.
31. Her Z, Tan JHL, Lim Y-S, Tan SY, Chan XY, Tan WWS, Liu M, Yong KSM, Lai F, Ceccarello E, et al. CD4+ T Cells Mediate the Development of Liver Fibrosis in High Fat Diet-Induced NAFLD

- in Humanized Mice. *Front Immunol.* 2020;11:580968. doi:10.3389/fimmu.2020.580968.
32. Pinyol R, Torrecilla S, Wang H, Montironi C, Piqué-Gili M, Torres-Martin M, Wei-Qiang L, Willoughby CE, Ramadori P, Andreu-Oller C, et al. Molecular characterisation of hepatocellular carcinoma in patients with non-alcoholic steatohepatitis. *J Hepatol.* 2021;75(4):865–878. doi:10.1016/j.jhep.2021.04.049.
 33. Villarreal DO, Allegranza MJ, Smith MA, Chin D, Luistro LL, Snyder LA. Targeting of CD122 enhances antitumor immunity by altering the tumor immune environment. *Oncotarget.* 2017;8(65):109151–109160. doi:10.18632/oncotarget.22642.
 34. Zhang Q, Huang H, Zheng F, Liu H, Qiu F, Chen Y, Liang C-L, Dai Z. Resveratrol exerts antitumor effects by downregulating CD8+CD122+Tregs in murine hepatocellular carcinoma. *Oncoimmunology.* 2020;9(1):1829346. doi:10.1080/2162402X.2020.1829346.
 35. Ochel A, Cebula M, Riehn M, Hillebrand U, Lipps C, Schirmbeck R, Hauser H, Wirth D. Effective intrahepatic CD8+ T-cell immune responses are induced by low but not high numbers of antigen-expressing hepatocytes. *Cell Mol Immunol.* 2016;13(6):805–815. doi:10.1038/cmi.2015.80.
 36. Ney JT, Schmidt T, Kurts C, Zhou Q, Eckert D, Felsher DW, Schorle H, Knolle P, Tüting T, Barchet W, et al. Autochthonous liver tumors induce systemic T cell tolerance associated with T cell receptor down-modulation. *Hepatology.* 2009;49(2):471–481. doi:10.1002/hep.22652.
 37. Mathews DV, Dong Y, Higginbotham LB, Kim SC, Breeden CP, Stobert EA, Jenkins J, Tso JY, Larsen CP, Adams AB. CD122 signaling in CD8+ memory T cells drives costimulation-independent rejection. *Journal of Clinical Investigation.* 2018;128(10):4557–4572. doi:10.1172/JCI95914.